American Mineralogist, Volume 61, pages 853–863, 1976

The chemical compositions and origin of the zeolites offretite, erionite, and levyne

WILLIAM S. WISE

Department of Geological Sciences, University of California
Santa Barbara, California 93106

AND R. W. TSCHERNICH

532 Avenue A
Snohomish, Washington 98920

Abstract

Since offretite, erionite, and levyne have similar structural elements, a chemical study of intergrowths from cavities in basalts was made in order to find chemical parameters that control the crystallization of each mineral. Chemical analyses were made of parts of a complex intergrowth of all three zeolites from Milwaukie, Oregon; of offretite overgrowths on levyne from British Columbia and Arizona; of erionite overgrowths from Rock Island Dam, Washington; and of intergrowths of offretite and erionite from Malpais Hill, Arizona, as well as of offretite and erionite from new localities in Oregon and Arizona. Erionite has Si/Al ratios between 3.6 and 3.0 with K + Na > Ca + Mg; offretite has Si/Al ratios between 2.8 and 2.3 with Ca + Mg > K + Na; and levyne has Si/Al ratios between 2.2 and 1.8, and Ca ≫ Na > K.

Compositional breaks in Si contents between each mineral indicate that their crystallization is controlled by the silica activity of the solution. The relatively common occurrence of erionite, rather than offretite, as a diagenetic mineral in siliceous tuffs is apparently related only to silica activity of the interstitial water. Compositions of the heulandite or clinoptilolite associated with offretite or erionite, respectively, have Si/Al ratios higher than the range of erionite, suggesting those zeolites result from even higher silica activities. K seems an essential constituent for offretite and erionite but not for levyne. Overgrowths of offretite on levyne require increases in activities of K and silica. Higher activities of K commonly result in the concurrent crystallization of phillipsite with offretite and erionite.

Introduction

During the past few years, various intergrowths of offretite, erionite, and levyne have been described, including zonal growths and stacking faults in offretite and erionite crystals (Sheppard and Gude, 1969; and Kokotailo *et al.*, 1972), offretite overgrowths on levyne (Sheppard *et al.*, 1974) and erionite on levyne (Passaglia *et al.*, 1974; Shimazu and Mizota, 1972). We have found and studied several more examples, including one intricate intergrowth of all three zeolites. By combining knowledge of growth sequences and results of detailed chemical studies with known crystal structure data, we can place some chemical controls on the origin of these zeolites.

The structures of the three zeolites all have in common hexagonal layers built of double 6-member rings of tetrahedra (D6R) linked by single 6-member rings (S6R). Different stacking sequences (Fig. 1) yield the different kinds of channels and cages in each of the frameworks. However, a change from one stacking sequence to another accounts for such features as stacking faults in erionite (Kokotailo *et al.*, 1972) and the oriented overgrowths on the basal planes of levyne.

Chemical compositions of the three minerals show consistent differences, even though the basic structural elements are the same. Typical cell contents can be represented by:

offretite $(K_2,Ca,Mg)_{2.5}Al_5Si_{13}O_{36} \cdot 15\text{–}16H_2O$ $Z = 1$

erionite $(K_2,Na_2,Ca,Mg)_{2.1}Al_{4.2}Si_{13.8}O_{36} \cdot 15H_2O$ $Z = 2$

levyne $(Ca,Na_2,K_2)_3Al_6Si_{12}O_{36} \cdot 18H_2O$ $Z = 3$

Erionite is the most common of these three zeo-

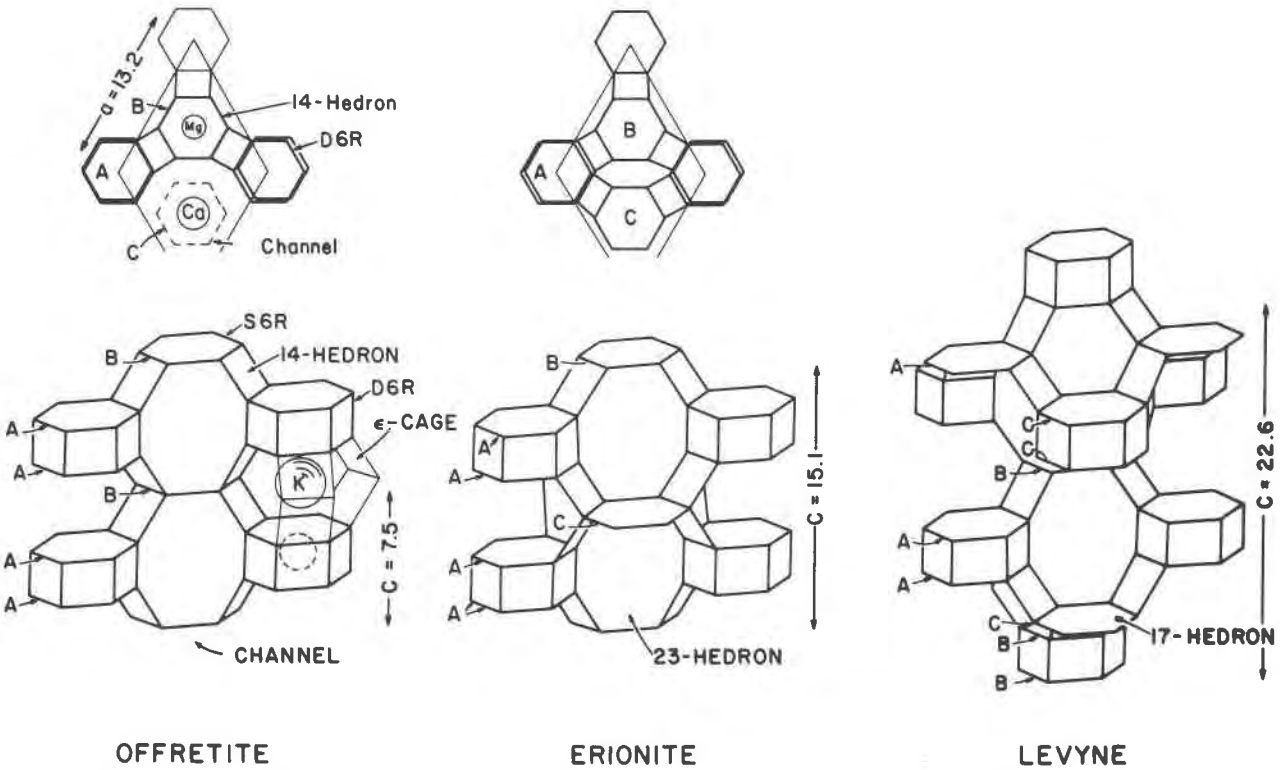

FIG. 1. Summary of the crystal structures of offretite, erionite, and levyne (after Gard and Tait, 1972; Breck, 1974; and Barrer and Kerr, 1959). All three structures are built of single 6-member rings of tetrahedra (S6R) arranged in various stacking sequences, but all retaining hexagonal symmetry.

Offretite. The S6R stacking sequence is *AABAAB* . . . , developing three kinds of cages: double 6-member rings (D6R) between successive *A* rings; ϵ cages (also called cancrinite cages) between successive D6R's; and 14-hedra (also called gmelinite-type cavities) between successive *B* rings. Cation locations: K^+ in ϵ-cages; a few Ca^{2+} in D6R's; hydrated Mg^{2+} in the 14-hedra; and hydrated Ca^{2+} in the wide channels. The space group is *P6m*2.

Erionite. The S6R stacking sequence is *AACAAB* . . . , giving a *c* dimension double that of offretite and developing three kinds of cages: D6R; ϵ cages; and 23-hedra between successive *B* rings and successive *C* rings. Cation locations: K^+ in ϵ cages; a few Ca^{2+} in D6R's; all others surrounded by water molecules in the very large 23-hedron. Space group symmetry is $P6_3/mmc$.

Levyne. The S6R stacking sequence is *BBCAABCCA* . . . , giving a *c* dimension three times that of offretite, and developing two kinds of cages: D6R, and 17-hedra, which are stacked in a one D6R and two 17-hedra sequence parallel to the *c* axis. Cation positions have not been determined. Space group symmetry is *R3m*.

lites, because it occurs as a diagenetic replacement of silicic tuffs as well as an amygdule mineral. Levyne forms in the cavities of basalts, such as those in the Columbia Plateau, Oregon; the Garron Plateau, Ireland; and the Deccan basalt of India. From our observations most levyne crystals have at least a thin, fibrous overgrowth of offretite. Offretite also occurs as single crystals or sprays of crystals in amygdules of alkalic, mafic lavas. Although the interpretation of zeolite sequences in cavities is tenuous, the relatively large crystals allow detailed chemical study of intergrowths, and thereby suggest some sequences of chemical changes during the formation of the different phases.

Experimental methods

All the chemical analyses in this study were performed by an electron probe microanalyzer on samples that ranged from relatively thick plates of levyne to fibrous growths of offretite. Whole clusters and intergrowths were embedded in epoxy and ground to expose the centers of crystals or intergrowths. Mounts were then polished and coated with approximately 250 Å of carbon. An accelerating voltage of 15 kV was used for all elements with a sample current of 10 nA. Standards used were andesine (Ca and Al), K-feldspar (K and Si), olivine (Mg), hematite (Fe), sanbornite (Ba), and celestite (Sr). Emission data

were reduced with a modified version of the computer program EMPADR 7 (Rucklidge and Gasparrini, 1969, Department of Geology, University of Toronto). In order to overcome some difficulties in analyzing zeolites by EMX methods, large beam diameters (10 to 20 micrometers) were used, the beam was moved after every 10-second counting period, and only the largest crystals or crystal clusters were analyzed. Where possible multiple spots were analyzed; the averaged results are listed in Table 1. Unit-cell contents calculated from these analyses are listed in Table 2.

Most of the samples were photographed with a scanning electron microscope; characteristic morphologies are illustrated in Figures 2 through 7. The samples were coated with 200 to 400 Å of AuPd. The thinner coats are less satisfactory because of some charging effects on thin needles.

If sufficient material was available, each sample was X-rayed to verify identification. However, offretite and erionite intergrowths can only be identified by the optical methods described by Sheppard and Gude (1969). Our chemical and X-ray data support

TABLE 1. Averaged microprobe analyses of offretite, erionite, levyne, and some associated zeolites

	1	2	3	4	5	6	7	8	9	10	11
SiO_2	57.07	54.00	54.97	55.73	55.97	55.99	47.91	55.78	50.29	56.44	57.21
Al_2O_3	16.43	18.76	17.70	20.62	19.94	20.62	23.31	20.79	22.18	20.04	17.10
Fe_2O_3	2.32	0.93	2.07	0.26	0.21	0.0	0.0	0.0	0.0	0.10	0.09
MgO	0.56	0.39	0.42	0.28	0.39	0.0	0.0	0.0	0.0	0.26	1.04
CaO	5.97	8.00	7.40	10.00	6.36	7.61	9.98	8.23	10.47	8.04	4.95
Na_2O	0.0	0.03	0.0	0.52	1.58	0.22	2.03	0.36	1.26	0.73	0.16
K_2O	2.39	2.58	2.34	0.84	4.06	3.81	0.48	5.53	1.42	3.22	4.66
Total:	84.74	84.69	84.90	88.25	88.51	88.25	83.71	90.69	85.62	88.83	85.21

	11p	11h	12	12p	12c	13	14	15	15p	15c	16
SiO_2	54.77	63.57	57.80	63.74	59.58	57.30	59.45	60.16	59.85	65.90	62.52
Al_2O_3	23.53	15.01	16.15	18.90	12.70	16.23	16.63	16.19	15.97	13.10	16.48
Fe_2O_3	0.03	0.08	0.08	0.08	0.02	0.02	0.0	0.10	0.0	0.04	0.01
MgO	0.10	1.48	0.97	0.0	0.56	1.17	0.34	0.88	0.0	0.06	1.12
CaO	4.67	4.53	5.26	3.72	3.28	4.62	4.91	5.34	2.56	4.41	2.49
SrO	0.0	0.56	0.0	0.0	0.0	0.0	0.0	0.0	0.0	0.0	0.0
BaO	1.09	0.15	0.0	0.56	0.0	0.0	0.0	0.0	1.67	0.42	0.0
Na_2O	0.54	0.0	0.59	3.08	0.79	0.17	0.57	0.20	2.71	0.58	1.72
K_2O	6.73	1.62	5.26	5.39	1.84	4.18	4.74	3.73	6.27	2.39	4.84
Total	91.14	87.00	86.11	95.67	78.79	83.69	86.64	86.60	89.03	86.90	89.18

1. Erionite in complex intergrowth (see figure 8c), quarry at corner of Lava and River Rds., Milwaukie, Ore.
2. Offretite in complex intergrowth (see figure 8c), quarry at corner of Lava and River Rds., Milwaukie, Ore.
3. Erionite with offretite in complex intergrowth (see figure 8c), quarry at corner of Lava and River Rds., Milwaukie, Ore.
4. Levyne in complex intergrowth (see figure 8c), quarry at corner of Lava and River Rds., Milwaukie, Ore.
5. Offretite in complex intergrowth (see figure 8c), quarry at corner of Lava and River Rds., Milwaukie, Ore.
6. Offretite on levyne, along Douglas Lake Rd., southwest of Westwold, s. British Columbia.
7. Levyne, along Douglas Lake Rd., southwest of Westwold, s. British Columbia
8. Offretite on levyne, along Queen Creek, 6 miles west of Superior, Pinal Co., Arizona
9. Levyne, along Queen Creek, 6 miles west of Superior, Pinal Co., Arizona
10. Offretite, road cut 2.1 miles s. of Owyhee Dam, Malheur Co., Oregon
11. Offretite (+erionite), railroad cut, n.e. side Malpais Hill, 6 miles s. Winkleman, Pinal Co., Arizona
11p Phillipsite, railroad cut, n.e. side Malpais Hill, 6 miles s. Winkleman, Pinal Co., Arizona
11h Heulandite, railroad cut, n.e. side Mailpais Hill, 6 miles s. Winkleman, Pinal Co., Arizona

12. Offretite, Rock Island Dam
12p Phillipsite, Rock Island Dam
12c Clinoptilolite, Rock Island Dam

13. Erionite,along new road cuts 0.1 mile north of Clifton, Greenlee County, Arizona

14. Erionite, blocks of basalt 2 miles north of Thumb Butte, eastern Graham County, Arizona

15. Erionite, quarry at Cape Lookout, Tallamook Co., Oregon
15p Phillipsite, quarry at Cape Lookout, Tillamook Co., Oregon
15c Clinoptilolite, quarry at Cape Lookout, Tillamook Co., Oregon

16. Erionite, Road cuts at Yaquina Head, Lincoln Co., Oregon

TABLE 2. Cell contents* and cell dimensions of analyzed offretites, erionites, and levynes

Sample Number	Mineral(s)	Locality	K	Na	Ca	Mg	Fe	Al	Si	a†	c†
1	erionite††	Milwaukie, Ore.	0.75	0.0	1.58	0.19	0.0	4.55	13.51		
2	offretite††	Milwaukie, Ore.	0.79	0.0	2.06	0.14	0.0	5.23	12.77		
3	erionite (+offretite)††	Milwaukie, Ore.	0.74	0.0	1.96	0.15	0.0	4.94	13.05		
4	levyne	Milwaukie, Ore.	0.24	0.23	2.40	0.10	0.01	5.46	12.51		
5	offretite	Milwaukie, Ore.	1.17	0.69	1.54	0.13	0.04	5.33	12.68		
6	offretite	near Westwold, B.C.	1.10	0.10	1.84	0.0	0.0	5.49	12.66	13.335(8)	
7	levyne	near Westwold, B.C.	0.15	0.94	2.57	0.0	0.0	6.59	11.50	13.386(5)	23.0(1)
8	offretite	near Superior, Az.	1.58	0.16	1.97	0.0	0.0	5.48	12.47		
9	levyne	near Superior, Az.	0.43	0.58	2.63	0.0	0.0	6.15	11.82		
10	offretite	Owyhee Dam, Ore.	0.92	0.32	1.94	0.09	0.02	5.31	12.83	13.315(1)	7.556(5)
11	offretite (+erionite)	Malpais Hill, Az.	1.38	0.07	1.23	0.36	0.02	4.69	13.30	13.278(8)	
12	offretite (+erionite)	Rock Is. Dam, Washington	1.57	0.27	0.98	0.34	0.02	4.46	13.53		
13	erionite	Clifton, Az.	1.26	0.08	1.17	0.41	0.01	4.50	13.50	13.280(3)	15.11(1)
14	erionite	Thumb Butte, Az.	1.38	0.25	1.20	0.11	0.0	4.48	13.58	13.283(3)	15.11(1)
15	erionite	Cape Lookout, Ore.	1.08	0.09	1.30	0.29	0.02	4.33	13.65	13.267(3)	15.11(3)
16	erionite	Yaquina Head, Ore.	1.36	0.74	0.59	0.37	0.0	4.28	13.78	13.245(2)	15.13(2)

* Based on 36 oxygens for all three minerals
† Except for samples 6 and 11, these are least squares refinements, the figure in parenthesis represents the calculated deviation applied to the figure immediately preceding it. Thus, 15.11(1) is 15.11 ±0.01.
††These cell contents have been corrected for included clay (iron-rich smectite) which ranged up to 2%.

their assertion that offretites are optically negative and erionites are optically positive.

The unit-cell dimensions listed in Table 2 were obtained by least-squares refinement of powder X-ray diffraction data, using the U. S. Geological Survey's FORTRAN IV computer program W7214. Silicon (Natl Bur. Stand. SRM 640, a = 5.43088 Å) was used as an internal standard for oscillations over the peaks listed by Sheppard and Gude (1969) and Sheppard *et al.* (1974). Since very small quantities of two samples (6 and 11) were available, the X-ray powder data could not be refined, and a was calculated from d_{400}.

Descriptions of analyzed samples

Milwaukie, Oregon

Intricate intergrowths of erionite, offretite, and levyne occur in some vesicles in basalt, exposed in a small quarry (now a vacant lot at the corner of Lava and River Roads, Milwaukie, Oregon). The basalt, a flow in the Yakima Basalt section west and south of Portland (Trimble, 1963), has a coarse, open texture without phenocrysts. Small crystals of stilbite and chabazite are common in the vesicles, but the erionite–offretite–levyne intergrowths are sparsely distributed.

There are five stages in the development of the intergrowths; most of the intermediate stages can be found in some vugs (Figs. 2–4). The cross section (Fig. 8c) was drawn from the section cut for microprobe analysis.

Stage 1. Erionite crystallized as needles clustered in the form of a tapering hexagonal prism (Point 1, Fig. 8c, and Analysis 1). Inclusions of an iron-rich smectite color these clusters pinkish orange. Identification of the erionite was made by both X-ray and optical methods.

Stage 2. Irregular crystals of offretite with some erionite interlayered with clay formed hollow, hexagonal cylinders, twice as high and enveloping the first stage prism (Fig. 2). The entire growth is in optical continuity, but the layers shown in Figure 8c as erionite have positive elongation, while the remainder is negative. Only the negative part (offretite) was analyzed as Point 2 (Analysis 2).

Stage 3. Compact subparallel needles overlie the open, porous growth of Stage 2. This zone (Figs. 3 and 4) includes less clay and is composed entirely of

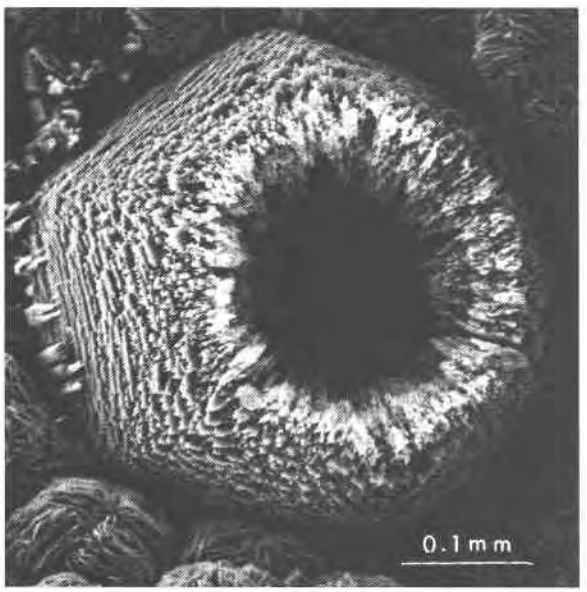

FIG. 2. Scanning electron micrograph of an offretite–erionite–clay (iron-rich smectite) intergrowth, Milwaukie, Oregon. The open intergrowth has all crystals in optical continuity and the *c* axes are nearly vertical.

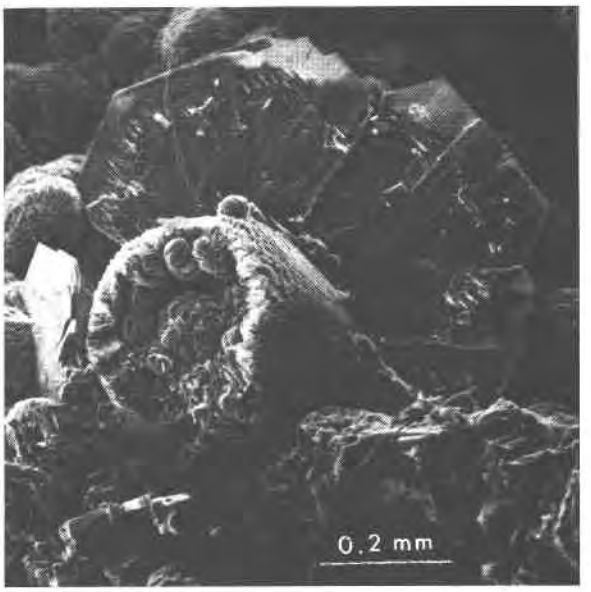

FIG. 3. Scanning electron micrograph of offretite–levyne intergrowth, Milwaukie, Oregon. The clay-filled cylinder is composed largely of offretite with some intergrown erionite, and the levyne plates have a thin overgrowth of offretite (white fibers).

erionite (identified by the positive elongation). Because this zone is so narrow, the analysis of a portion of this zone (Analysis 3) probably includes some offretite.

Stage 4. Thin plates of levyne (about 0.05 mm thick, Analysis 4) grew from the base of the core cylinder outward at least 0.5 mm. There are several specimens of multiple, parallel plates; however, those shown in Figure 3 are typical. The *c* axes of the levyne and earlier-formed erionite and offretite are parallel.

Stage 5. An overgrowth of very thin offretite fibers (Analysis 5) added as much as 0.1 mm to all the exposed parts of the intergrowth. Figure 4 illustrates the long, wispy needles in an early part of this stage. Continued growth would cover this exposed surface, giving it an appearance like that in Figure 5. Identification of this offretite was based on its negative elongation.

The balls of plates in Figure 2 and 3 are iron-rich smectite that recrystallized after stage 5 of zeolite growth.

Offretite overgrowths on levyne

New localities with particularly striking offretite overgrowths on levyne have been found southwest of Westwold, along the road to Douglas Lake, southern British Columbia, and along Queen Creek, 6 miles west of Superior, Pinal County, Arizona. The Westwold offretite overgrowths are extraordinarily thick, 1.0 mm on levyne plates 0.2 mm thick (Analyses 6 and 7). Although scarce, the Queen Creek overgrowths are exceptional in that they are thin on rela-

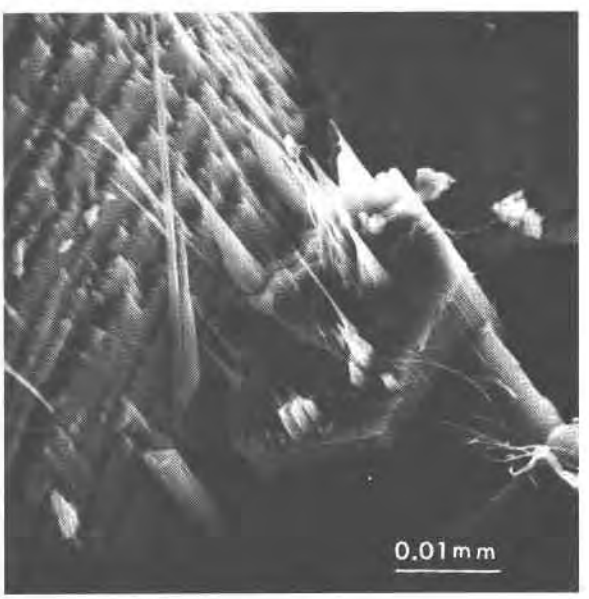

FIG. 4. Scanning electron micrograph of offretite–levyne intergrowth, Milwaukie, Oregon. (Detailed view of part of Fig. 3.) The view shows the join between the levyne plate and the offretite core cylinder, but with long fibers of offretite overgrowing both earlier formed structures.

FIG. 5. Scanning electron micrograph of offretite overgrowths on levyne from Queen Creek, near Superior, Arizona. Note that the offretite fibers have grown only on the basal faces of the levyne.

tively thick levyne (Fig. 5), and clearly show growth only on the basal planes (Analyses 8 and 9).

Owyhee Dam, Oregon

Fibers of offretite forming hexagonal prisms occur sparsely at Owyhee Dam, Malheur County, Oregon (see Staples *et al.*, 1973, p. 406, for a description of the locality and host rock). The prisms are about 0.3 × 1.0 mm and are composed entirely of offretite (Analysis 10).

Offretite–erionite intergrowths

Particularly interesting occurrences of offretite with erionite intergrowths are found at Malpais Hill, 6 miles south of Winkleman, Pinal County, Arizona, and two miles south of Horseshoe Dam, Maricopa County, Arizona. Malpais Hill is a Plio-Pleistocene olivine basalt volcano that erupted subaqueously in a shallow lake. Vesicular blocks, colored orange by the hydrated and oxidized glass, contain vugs that are lined with celadonite and montmorillonite, which are in turn covered by small crystals of offretite, heulandite, and phillipsite. The Horseshoe Dam locality is a bed of river gravels containing orange vesicular cobbles of olivine basalt having the same mineralogy as the Malpais Hill basalt.

The Malpais Hill offretite crystals are sharp, hexagonal prisms about 0.1 mm long (Fig. 6). However, the crystals are actually intergrowths of offretite and erionite; the zones shown in Figure 8a were identified by the sign of elongation. The analyzed spots (Analysis 11) undoubtedly included several of the narrow erionite bands, and therefore represent an average for the crystal. The cell parameters from X-ray diffraction data likewise represent averages.

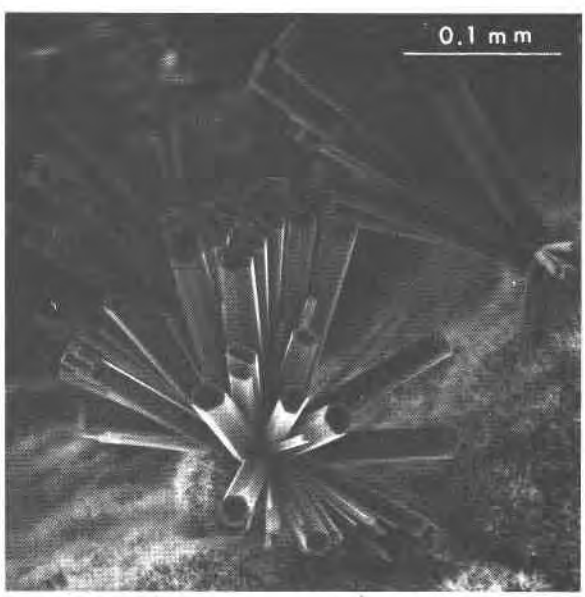

FIG. 6. Scanning electron micrograph of offretite from Malpais Hill, Pinal County, Arizona. The hexagonal prisms actually are intergrown offretite and erionite (see Fig. 8a), growing on celadonite.

FIG. 7. Scanning electron micrograph of erionite from Cape Lookout, Tillamook County, Oregon. The clusters of striated prisms are typical of erionite crystals having grown in basalt cavities.

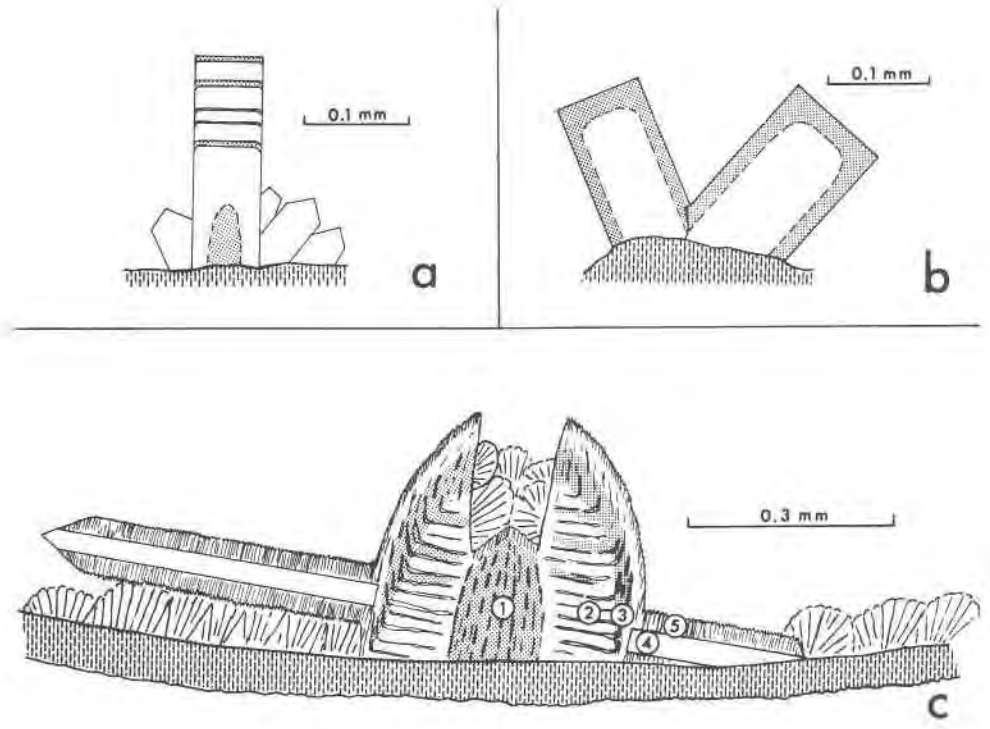

FIG. 8. Sketches of offretite–erionite–levyne intergrowths.
(a) Alternating erionite (shaded) and offretite in a stacking fault arrangement (associated with phillipsite), Malpais Hill, Arizona.
(b) Overgrowth of erionite (shaded) on offretite from Rock Island Dam, Washington.
(c) The complex intergrowths of offretite–erionite (shaded)–levyne, Milwaukie, Oregon. The numbers refer to stages of growth and to analyses in Tables 1 and 2. (1) erionite with clay, (2) offretite with clay and erionite, (3) erionite, (4) levyne, and (5) offretite overgrowth.

Zonal growths of offretite and erionite within a single crystal occur at Rock Island Dam, Washington, which is the type locality of paulingite, described by Kamb and Oke (1960). This growth (Fig. 8b) is similar to that observed in some offretite crystals from Mt. Simiouse near Montbrison, Loire, France (Sheppard and Gude, 1969). Again the analyses of these crystals (Analysis 12) probably represent an average of the two minerals. Long, very thin fibers of erionite also occur in the same rocks. Complete analysis on these fibers, about 5 μm in diameter, were not obtained, but K:Na:Ca is approximately 50:30:20, typical of many erionites but far more soda-rich than the offretite crystals.

Erionite localities

Two localities in southeastern Arizona (near Clifton, Greenlee County, and 2 miles north of Thumb Butte, Graham County) have yielded erionite in vesicles of mid-Tertiary olivine basalts. The erionite forms bundles and sprays up to 2 mm in length (Analyses 13 and 14). Common associated minerals are opal, quartz, mordenite, clinoptilolite, and phillipsite.

Erionite also occurs in amygdules of Miocene tholeiitic basalts in two localities along the coast of Oregon at Cape Lookout, Tillamook County (Analysis 15 and Fig. 7), and at Yaquina Head, Lincoln County (Analysis 16). The zeolite assemblage at Cape Lookout is complex but includes mordenite, clinoptilolite, phillipsite, and dachiardite. The Yaquina Head erionite occurs with clinoptilolite.

Discussion

As with most zeolites, the chemical compositions of these three minerals are nonstoichiometric and can be characterized by the Si/Al ratio in the framework and the content of the charge-balancing cations. Figure 9, a plot of the relationships between the Si content and the relative proportions of monovalent and divalent cations, shows that the three phases differ mainly with respect to their Si/Al ratios. The fields

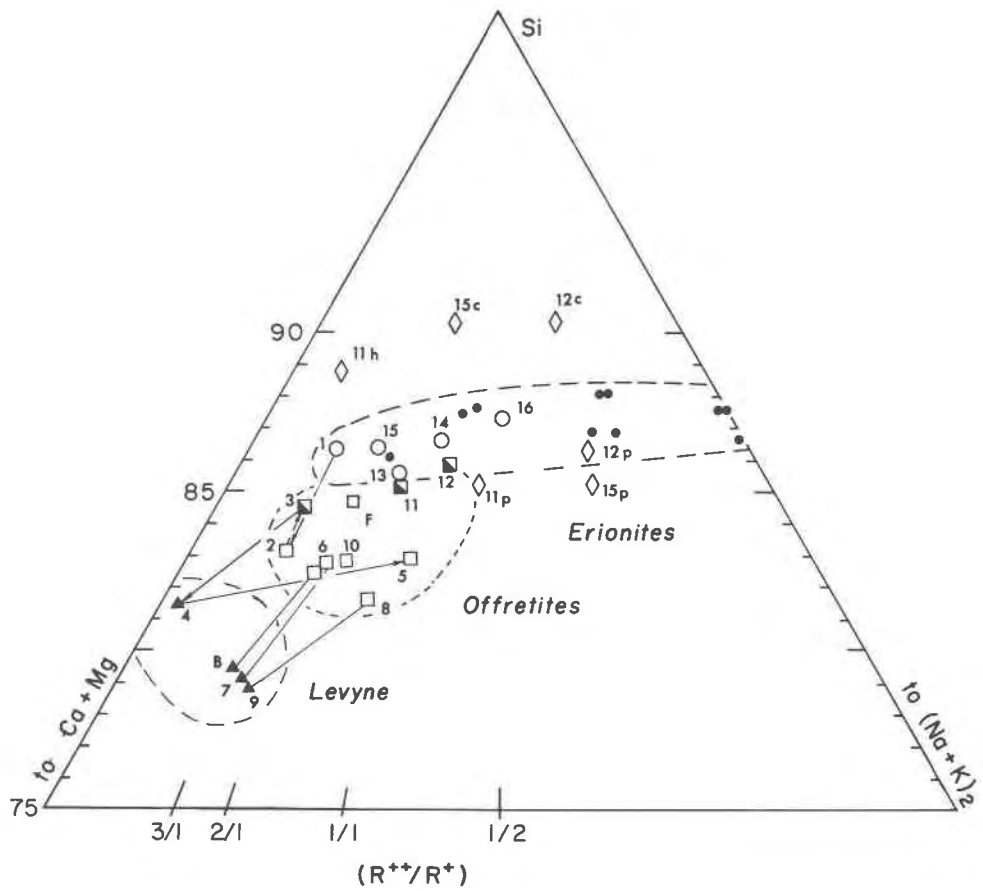

FIG. 9. Plot of Si–(Ca + Mg)–(Na_2 + K_2) of the analyzed minerals in Table 1. Numbers correspond to analyses. Circles are erionites (solid circles are from Sheppard and Gude, 1969), squares are offretite (half-filled squares are intergrowths of offretite and erionite). Triangles are levynes. Arrows connect the growth sequence of the Milwaukie intergrowths, and lines connect the offretite overgrowth with the host levyne. Sample B is Beech Creek, Oregon, offretite–levyne (Sheppard *et al.*, 1974); Sample F is original offretite, Montbrison, France (Sheppard and Gude, 1969). Diamonds labeled *p*, *h*, or *c* indicate associated phillipsite, heulandite, or clinoptilolite, respectively.

for offretite and erionite may overlap, but if Points 3, 11, and 12 represent analyses of mixtures (Figs. 8a and 8b), a miscibility gap may exist. The sharpness with which the phases can be distinguished optically suggests that gradations between the phases do not occur. We conclude, therefore, that the different stacking sequences are accompanied and probably controlled by differences in the Si/Al ratio. The analyses of the offretite and levyne intergrowths demonstrate a significant compositional gap.

The Si variation in the erionite field is small (13.5 silicons per 36 oxygens at Clifton, Arizona, to 14.1 per 36 in a sedimentary erionite from Malheur County, Oregon, giving Si/Al values between 3.0 and 3.6), but there is a wide variation in the relative proportions of divalent and monovalent cations (R^{++}/R^{+} ratio). Offretite compositions are somewhat more restricted; Si varies from 13.3 in those crystals intergrown with erionite to 12.0 in overgrowths on levyne, giving Si/Al ratios of 2.0 and 2.8; R^{++}/R^{+} varies only between 2/1 and 1/1. The levynes plotted here vary from 11.5 and 12.4 Si per cell, giving Si/Al ratios of 1.7 to 2.2, and have a great predominance of divalent cations.

Table 2 and the analyses in Sheppard and Gude (1969) show that the sum of all non-framework cations varies between 2.5 and 4.0, with values near 3 most common. Moreover, the crystal structure work of Gard and Tait (1972), illustrated in Figure 1, shows that a single layer within any of these structures has room for only four cations. An average erionite with 4 Al and therefore a framework charge

of −4 can be balanced with any combination of non-framework cations, including 4 monovalent ones. As the framework charge increases with decreasing Si content, more divalent cations are required to balance the charge, without exceeding the limit of four cations.

Since Al is mostly in the D6R cages (Gard and Tait, 1972), the *a* dimension of the unit cell is responsive to the Al substitution (Fig. 10). The trend for each mineral is generally the same, although the best-fit lines are not coincident.

Figure 11, a plot of Ca + Mg, Na, and K, shows that erionite has a wide range of compositions but generally with K + Na > Ca + Mg. The offretite field has Ca + Mg > K + Na, while the levynes have Ca >> Na > K. The new data support the generalizations made by Sheppard and Gude (1969) that most offretites contain very little Na, and that erionites and offretites contain at least 0.75 K per layer.

It is also clear from Figure 11 that erionites with very little Na also exist, and therefore the formation of the erionite or offretite framework does not depend on Na content. The occurrence of erionite rather than offretite as a diagenetic mineral in siliceous tuffs is dependent only on silica activity, which is controlled to a large extent by the tuff composition and the pH of the water.

The experimental work of Aiello and Barrer (1970) and the structural studies of Gard and Tait (1972) indicate that "each cancrinite cage (ϵ-cage) 'collects' around the K ion as a precursor to crystallization, and the frame is subsequently built up by condensation of these cancrinite cages" (Gard and Tait, 1972, p. 832). Table 2 and Figure 11 show that levyne contains very little K, which can be explained by the lack of ϵ-cages in the levyne structure.

Two other zeolite minerals intimately associated with erionite and offretite in the assemblages studied here are heulandite or clinoptilolite and phillipsite (Fig. 9). The heulandite and clinoptilolite with higher Si/Al ratios are clearly the result of increases in silica activity beyond values that erionite is able to accommodate. The associated phillipsites, having nearly the same Si/Al ratio, are probably responding to some other variable, such as high a_{K^+} or low a_{H_2O}.

Implications for natural zeolite growth

In an earlier paper (Wise and Tschernich, 1976), we argued that the activities of SiO_2 and H_2O are the principal variables that control the crystallization of high-silica zeolites. The compositional gap with respect to Si that probably exists between erionite and offretite suggests that again a_{SiO_2} plays a primary role. Since cation composition fields overlap, activities of these cations are apparently not important. Any two of the structures do not seem able to grow contempo-

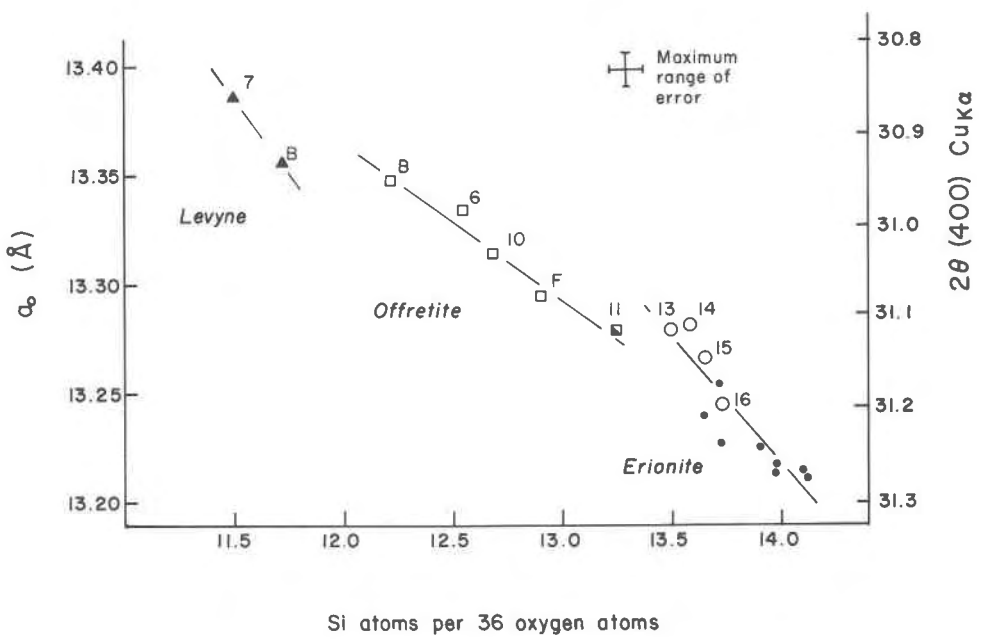

FIG. 10. Variation of the *a* dimension with Si content of the unit cell, based on 36 oxygens. Symbols are the same as in Fig. 9. Error bars represent plus and minus one standard deviation. The 400 peak appears only in offretite and erionite patterns.

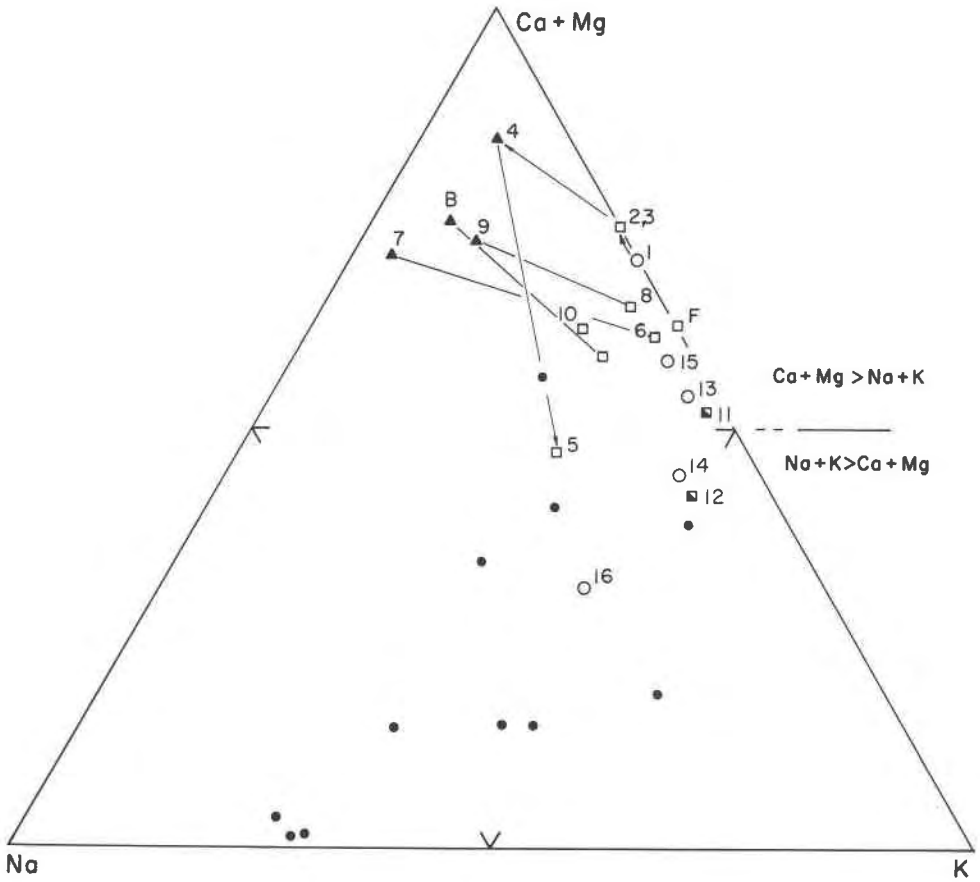

FIG. 11. (Ca + Mg)–K–Na plot of offretite, erionite, levyne. The symbols and lines are the same as Fig. 9.

raneously from the same solution. The reason why the Si/Al ratio affects the stacking sequence is not known, but the problem probably could be solved by determining Al locations in all three zeolites. For example, if the 6 Al's in levyne only occur in the D6R groups, the negative framework charge around these cages may be too strong to be shielded by cations forming ϵ cages. Therefore, lower structural energies are obtained by rotation of D6R cages (Fig. 1).

From the data presented here and the experimental work of Aiello and Barrer (1970), it is reasonably clear that K^+ is necessary to form the ϵ-cages prior to framework construction of offretite on levyne, and the crystallization of offretite may be a response to increases in either a_{SiO_2} or a_{K^+} or both. The crystallization of levyne (low Si/Al and low K) can cause increases in these constituents.

Acknowledgments

We are greatly indebted to Mr. Robert Mudra of Mesa, Arizona, for generously providing samples and showing us the Arizona zeolite localities he has found. Mr. and Mrs. Robert Hillsdon provided samples of the British Columbia zeolites. We appreciate the discussions and suggestions of Dr. James Boles concerning zeolite crystallization. Thanks also go to the Research Committee, University of California, Santa Barbara, for computer time used for reduction of microprobe and X-ray diffraction data.

References

AIELLO, R. AND R. M. BARRER (1970) Hydrothermal chemistry of silicates. Part XIV. Zeolite crystallization in presence of mixed bases. *J. Chem. Soc. (A)*, 1470–1475.

BARRER, R. M. AND I. S. KERR (1959) Intracrystalline channels in levynite and some related zeolites. *Trans. Faraday Soc.* **55,** 1915–1923.

BRECK, D. W. (1974) *Zeolite Molecular Sieves,* John Wiley and Sons, New York, 771 p.

GARD, J. A. AND J. M. TAIT (1972) The crystal structure of the zeolite offretite, $K_{1.1}Ca_{1.1}Mg_{0.7}$ $[Si_{12.8}Al_{5.2}O_{36}]$ · 15.2 H_2O. *Acta Crystallogr.* **B 28,** 825–834.

KAMB, W. B. AND W. C. OKE (1960) Paulingite, a new zeolite, in association with erionite and filaform pyrite. *Am. Mineral.* **45,** 79–91.

KOKOTAILO, G. T., S. SAWRUK AND S. L. LAWTON (1972) Direct

observation of stacking faults in the zeolite erionite. *Am. Mineral.* **57,** 439–444.

PASSAGLIA, E., E. GALI AND R. RINALDI (1974) Levynes and erionites from Sardinia, Italy. *Contrib. Mineral. Petrol.* **43,** 253–259.

SHEPPARD, R. A. AND A. J. GUDE, 3RD (1969) Chemical composition and physical properties of the related zeolites, offretite and erionite. *Am. Mineral.* **54,** 875–886.

———, ———, G. A. DESBOROUGH AND J. S. WHITE, JR. (1974) Levyne-offretite intergrowths from basalt near Beech Creek, Grant County, Oregon. *Am. Mineral.* **59,** 837–842.

SHIMAZU, M. AND T. MIZOTA (1972) Levyne and erionite from Chojabaru, Iki Island, Nagasaki Prefecture, Japan. *J. Jap. Assoc. Mineral. Petrol. Econ. Geol.* **67,** 418–424.

STAPLES, L. W., H. T. EVANS, JR. AND J. R. LINDSAY (1973) Cavansite and pentagonite, new dimorphous calcium vanadium silicate minerals from Oregon. *Am. Mineral.* **58,** 405–411.

TRIMBLE, D. E. (1963) Geology of Portland, Oregon and adjacent areas. *U. S. Geol. Surv. Bull.* **1119,** 119 p.

WISE, W. S. AND R. W. TSCHERNICH (1976) Chemical composition of ferrierite. *Am. Mineral.* **61,** 60–66.

Manuscript received June 6, 1975;
accepted for publication October 14, 1975.